

## Oceanic and orogenic fluid–rock interaction in $^{18}\text{O}/^{16}\text{O}$ -enriched metagabbros of an ophiolite (Tinos, Cyclades)

Benita Putlitz<sup>a,1</sup>, Yaron Katzir<sup>b,\*</sup>, Alan Matthews<sup>a</sup>, John W. Valley<sup>b</sup>

<sup>a</sup> Institute of Earth Sciences, The Hebrew University of Jerusalem, Jerusalem 91904, Israel

<sup>b</sup> Department of Geology and Geophysics, University of Wisconsin, 1215 W. Dayton St., Madison, WI 53706, USA

Received 15 April 2001; received in revised form 30 August 2001; accepted 7 September 2001

### Abstract

Two spatial scales of fluid–rock interaction in an ophiolite suite are revealed by oxygen isotope and hydrogen isotope studies of metagabbros on the island of Tinos (Cyclades, Greece). Sequentially formed mineral generations in the metagabbros include relict igneous augite, hornblende of sub-seafloor hydrothermal origin, and actinolite and albite formed by regional greenschist-facies metamorphism during orogenesis. With the exception of augite ( $\delta^{18}\text{O} = 4.4\text{--}5.6\text{‰}$ ), the metagabbros are characterized by unusually high  $\delta^{18}\text{O}$  values: hornblende ( $5.8\text{--}7.4\text{‰}$ ), actinolite ( $6.5\text{--}10.2\text{‰}$ ), feldspar ( $14.6\text{--}14.9\text{‰}$ ) and whole rocks ( $7.0\text{--}10.5\text{‰}$ ). Hornblende  $\delta D$  values range from  $-57$  to  $-66\text{‰}$ . The high  $\delta^{18}\text{O}$  values and the  $\delta D$  range of the hornblendes are compatible with interaction of oceanic gabbro with seawater that had previously been enriched in  $^{18}\text{O}/^{16}\text{O}$  ( $\delta^{18}\text{O} = 6.5\text{--}8\text{‰}$ ) by isotopic exchange at moderate to high temperatures. The high degree of oceanic alteration in the layered gabbros, mass balance calculations of isotopic exchange, and field evidence for early oceanic thrusting suggest that seawater could have penetrated deeply into the ocean crust, becoming  $^{18}\text{O}/^{16}\text{O}$ -enriched through isotopic exchange with gabbros at progressively increasing temperature. Upward, down-temperature flow of the high- $\delta^{18}\text{O}$  water would be very effective in elevating the  $\delta^{18}\text{O}$  values of gabbros. The regional greenschist metamorphic overprint of the ophiolite, possibly the result of continued thrusting and piling up of nappes during obduction, is characterized by localized fluid–rock exchange. Actinolite in massive gabbroic layers has  $\delta^{18}\text{O}$  values ( $6.5\text{--}7.2\text{‰}$ ) close to those of the hornblende, whereas in deformed meter-sized gabbroic blocks the amphiboles have significantly higher values ( $8.4\text{--}10.2\text{‰}$ ). Likewise, albite in the gabbroic blocks has high  $\delta^{18}\text{O}$  values of ca.  $15\text{‰}$  that are ascribed to meter-scale exchange with  $^{18}\text{O}$ -rich fluids derived from dehydration reactions in low-temperature hydrothermally altered basaltic host rock enclosing the blocks. Deformation-enhanced permeability facilitated fluid infiltration in gabbroic blocks, whereas the relatively undeformed, and therefore less permeable, massive gabbros experienced minor interaction with fluids. The orogenic fluid–rock interaction thus represents local-scale redistribution of hydrous mineral components introduced during seafloor hydrothermal exchange. © 2001 Elsevier Science B.V. All rights reserved.

**Keywords:** gabbros; ophiolite; O-18/O-16; Cyclades; metamorphism

\* Corresponding author. Tel.: +1-608-2627118; Fax: +1-608-2620693. E-mail address: yaron@geology.wisc.edu (Y. Katzir).

<sup>1</sup> Present address: Institut für Geowissenschaften, Universität Potsdam, Postfach 60 15 53, D-14415 Potsdam, Germany.

## 1. Introduction

Stable isotope studies of fresh ocean crust and ancient ocean crust preserved in ophiolites have provided important insight into the processes of hydrothermal seawater–rock interaction occurring at oceanic spreading centers [1–4]. Typically, it is found that gabbros have  $\delta^{18}\text{O}$  values lower than that of unaltered MORB ( $5.7 \pm 0.2\%$ ) [5,6] as a result of moderate to high temperature exchange with seawater. In contrast, low-temperature alteration seen in the upper parts of the extrusives from ophiolites and ocean crust sections results in relatively high  $\delta^{18}\text{O}$  values of up to 13‰ (e.g. [6]). Having been transported to convergent margins by plate motion, hydrothermally altered ocean crust may be either subducted or obducted on one of the colliding plates. In either case, metamorphism may occur and seawater incorporated into the oceanic rocks by seafloor hydrothermal alteration will become a potentially important source of hydrous metamorphic phases and thereby influence the fluid–rock interaction history during metamorphism.

Metamorphosed oceanic basalts, gabbros and ultramafics in the Alpine orogen of the Cyclades occur in both high-pressure metamorphic sequences and in ophiolitic sections that were imbricated at higher structural levels without undergoing high-pressure metamorphism. The Eocene high-pressure metamorphic event was attributed to the closure of the Mesozoic Pindos ocean basin by subduction of the Apulian microplate, and eventual collision with the Eurasian continent [7,8]. The types of protoliths and the tectonic duplication of the high-pressure metamorphic sequences of the northwestern Cyclades islands suggest that they form part of a subducted accretionary wedge [9]. Thus, the high-pressure metamorphosed basaltic–gabbroic–ultramafic association might represent fragments of the floor of the Neo-Tethyan Pindos ocean that were incorporated into the wedge during a subduction accretion process. Similarly, the ophiolitic association found in sequences that tectonically overlie the high-pressure metamorphic rocks might also represent obducted and metamorphosed Pindos seafloor. These two different ophiolitic associa-

tions provide the opportunity for understanding fluid–rock interaction during seafloor alteration and metamorphism of Tethyan ocean floor.

The oceanic and orogenic fluid–rock interaction history of the metamorphosed obducted ophiolites is investigated in this work through oxygen isotope and hydrogen isotope studies of the metagabbros of the island of Tinos (Fig. 1). Previous studies of the field relations, petrology and geochemistry [10] showed that the Tinos ophiolite exposures represent a sliced and dismembered ophiolite complex, which had undergone hydrothermal seafloor alteration and a pervasive regional metamorphic overprint in the greenschist facies. The metagabbros preserve mineral relics of each of these processes, allowing examination of the seafloor fluid–rock interaction leading to the creation of hydrothermal mineralogy and the subsequent modification of this mineralogy during metamorphism. The research complements an isotopic study of the high-pressure metamorphic gabbros and basalts of the islands of Syros, Sifnos and Tinos [11], which showed that the high-pressure minerals of the gabbros and basalts (garnet, glaucophane, omphacite, epidote) reflect the whole-rock stable isotope composition of the precursor seafloor hydrothermal alteration processes. Minerals in metagabbros inherit the low  $\delta^{18}\text{O}$  values typical of deeper-seated high-temperature seafloor alteration, whereas the minerals in metabasalts have high  $\delta^{18}\text{O}$  values, reflecting low-temperature alteration of extrusive rocks.

## 2. Geological setting and evolution of the Tinos ophiolite

The Alpine orogen of the Cyclades consists of two main tectonic units: the lower tectonic unit (LTU) comprising rocks that underwent subduction and high-pressure metamorphism at Late Cretaceous–Eocene times [12,13], and the upper tectonic unit (UTU) containing a variety of metamorphosed and unmetamorphosed rock sequences that were not subducted (Fig. 1). The crystalline geology is completed by the extensive exposures of Miocene granitoids (Fig. 1) [12,14].

The LTU in the NW Cyclades consists of meta-

morphosed sedimentary and volcanic sequences including thin intervals of ophiolitic mélanges [9,14,15]. The peak  $P$ – $T$  conditions of the Eocene HP metamorphism have been estimated at about  $15 \pm 5$  kbar and  $480 \pm 30^\circ\text{C}$  [12,16,17]. The high-pressure metamorphic assemblages were overprinted by greenschist-facies metamorphism at similar temperatures, but pressures of 5–7 kbar, at Oligocene–Miocene times [12,18].

The UTU is very heterogeneous and comprises unmetamorphosed and medium- to low-pressure metamorphic rocks, including Miocene clastic sequences, unmetamorphosed Jurassic ophiolite, and Late Cretaceous greenschist- and amphibolite-facies metamorphosed ophiolitic mélange and volcano sedimentary sequences ([14,19] and references cited therein).

Both tectonic units are exposed on Tinos (Fig. 1) and were juxtaposed by a low-angle normal fault that was active as early as Early Miocene time [20–23]. The UTU on Tinos comprises a dismembered ophiolite suite that includes the metagabbros studied in this work. The following history was deduced for the ophiolite [10]: (1) Ocean crust was generated at a Mesozoic [24] Tethyan spreading center and underwent low-temperature seafloor alteration of basalts and high-temperature alteration of gabbros. Deeper ultramafic rocks were not affected by high-temperature hydrothermal metamorphism, but later were tectonically brought into direct contact with seawater and underwent low-temperature serpentinization. (2) Tectonism after cooling involved thrusting that caused repetition and inversion of the original order of the oceanic suite. (3) Regional metamorphism of all ophiolitic components at greenschist-facies conditions (ca.  $450^\circ\text{C}$ ) overprinted the earlier hydrothermal alteration mineralogy, and is often accompanied by penetrative deformation. Regional metamorphism might have been induced by continued thrusting and piling up of nappes during obduction. The similarity in structures and metamorphic grade between mafic phyllites of the UTU and underlying greenschists of the LTU was taken to conclude that both units were metamorphosed together in the Oligocene–Miocene times [22]. Recent Rb–Sr and  $^{40}\text{Ar}/^{39}\text{Ar}$  studies indicate that the UTU underwent Ar and

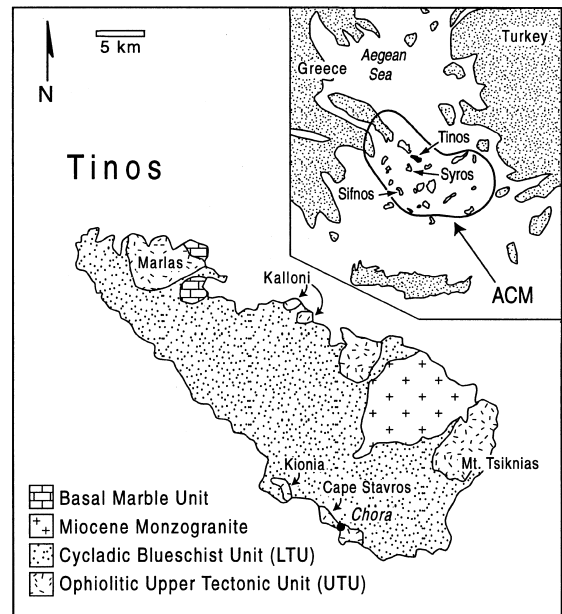


Fig. 1. Geological map of Tinos island (Cyclades, Greece) showing the ophiolite exposures (UTU) and sample locations. ACM, Attic Cycladic Massif.

Rb–Sr age resetting during ductile extension at 25–21 Ma [24,25].

The present-day stratigraphic section consisting of tens of meters thick slices of mafic phyllites (basalts) overlain by serpentinites and gabbros is considered to have been derived by a combination of thrusting during obduction and subsequent attenuation by low-angle normal faulting. Two major metagabbro types are readily identified in the field [10]: massive *layered metagabbros* forming coherent layers at Mount Tsiknias and Cape Stavros exposures and deformed *metagabbroic blocks* enclosed in mafic (metabasaltic) phyllitic (Fig. 2a) and calcareous metasedimentary or ultrabasic (serpentinite) country rocks at the Kalloni, Kionia and Marlas exposures.

The *massive metagabbros* are characterized by hornblende and plagioclase-rich bands, which resemble original magmatic layering. Primary igneous augite and Cr-spinel are still preserved. The augite is typically replaced by brown or green magnesiohornblende [10], indicating very high degree of hydrothermal alteration (up to 100% in some samples). This hornblende is in turn fre-

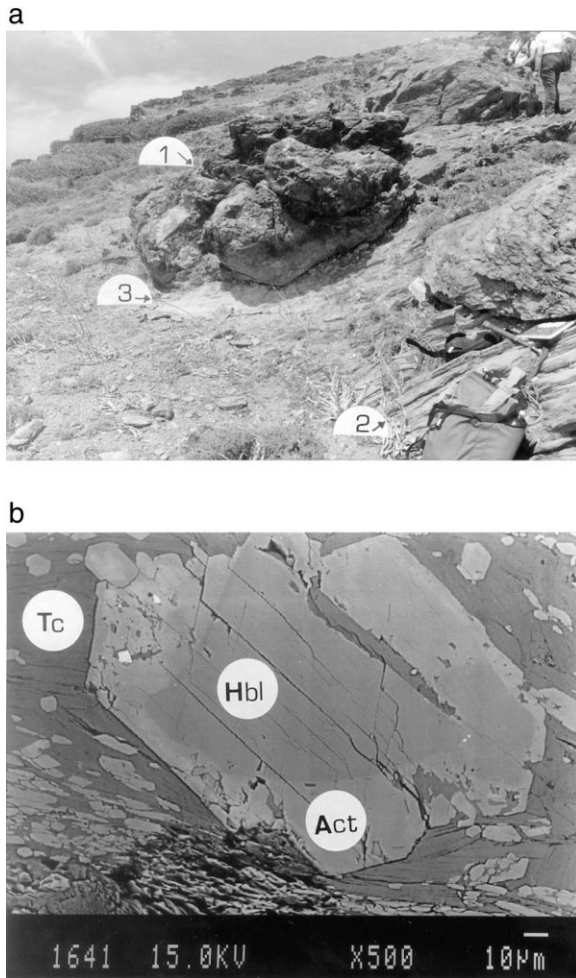


Fig. 2. a: Field setting of the metagabbroic block of Kionia. The block of metagabbro (1) is enclosed within strongly foliated mafic phyllites (2). A light-colored tremolite–chlorite contact zone (3) implies that the tectonic admixture preceded metamorphism. b: Zoned porphyroblast of amphibole in a sheared talcaceous matrix. Core of hornblende (Hbl) is rimmed by actinolite (Act). Actinolite and talc (Tc) represent greenschist-facies conditions that prevailed during regional metamorphism and deformation. The hornblende is a relict of an earlier high-temperature event. This sample from a sheared gabbro elegantly illustrates the textural relations between hornblende and overprinting actinolite.

quently replaced by actinolitic amphibole (Fig. 2b), which together with clinozoisite, chlorite and albite form the greenschist-facies assemblage of the metagabbro. In some cases, direct reaction of augite to the greenschist-facies minerals chlorite and actinolite is observed.

Deformation and the greenschist-facies overprint are more prominent in the metagabbroic blocks, often leaving only relics of the older hornblende in an oriented fine-grained greenschist matrix. The compositional range of amphibole is more restricted than in the gabbro layers varying from low-Al magnesiohornblende and actinolitic hornblende to actinolite or tremolite.

Oxygen isotope studies of metabasalts of the LTU on Tinos show that high-pressure metamorphism [11] and the Oligocene–Miocene greenschist overprint [12,26] occurred at low water/rock ratios. The metabasaltic rocks and minerals have high  $\delta^{18}\text{O}$  values ( $> 10\text{‰}$ ) reflecting the inheritance of the isotopic compositions from earlier low-temperature seafloor alteration [11,26]. Preliminary oxygen isotope studies of whole-rock samples of metabasalts and serpentinites of the UTU ophiolitic unit [10] also showed high  $\delta^{18}\text{O}$  values. Despite their different metamorphic histories, the Tinos UTU metagabbros feature many similarities to their LTU counterparts on Syros. Relict hydrothermal amphiboles are preserved and the exposures on both islands consist of massive metagabbroic bodies as well as smaller meter-size boulders.

### 3. Methods

The very fine scale of intergrowth among the different mineral generations required careful separation procedures. In samples where only small amounts of pure mineral could be separated, advantage was taken of the ability of the laser probe system to routinely analyze 1–2 mg of material. Portions or slabs of each sample, usually a few hundred grams, were crushed and sieved, and concentrates were produced by mechanical methods (magnetic Frantz separator, air-abrasion-mill or vibration table). Between 2 and 3 mg of material was handpicked from the concentrates for oxygen isotope analyses (usually with grain-sizes between 100 and 500  $\mu\text{m}$ ). In some cases, hand-samples were sectioned according to their layering or zoning, and each layer or zone was individually processed. Whole-rock samples were powdered to  $< 150 \mu\text{m}$  for analysis.

Table 1  
Oxygen and hydrogen isotopic compositions of metagabbros and host rocks from Tinos, Greece

Sample no.	Rock type	$\delta^{18}\text{O}$ ‰ SMOW					$\delta D$ ‰ SMOW	
		Igneous CPX	Hornblende		Actinolite	Whole rock		Others
			Green	Brown				
Mount Tsiknias, massive layered gabbros								
TC 3	MG		6.66 ± 0.04 (3)	6.52 ± 0.21 (3)	7.18 ± 0.10 (2)	7.07		
EX 6	MG	4.47 ± 0.08 (2)	5.84 ± 0.02 (2)				FV 5.27 ± 0.09 (2)	
Ti 39	MG	5.49 ± 0.18 (2)						
Ti 34	MG						Hbl -66.3 ± 6.9 (2)	
EX 5	QV						Qtz 12.19 ± 0.31 (2) Ep -59.1	
Cape Stavros, massive layered gabbros								
TT 49	MG			6.31 ± 0.08 (3)				
TT 55	MG		6.27 ± 0.02 (2)	5.75 ± 0.10 (5)	6.99	6.99		
Ti 51	MG		5.48 ± 0.13 (2)	6.45	6.50		Hbl -66.2 ± 2.8 (2)	
TT 51	MG					9.59	Hbl -69.0	
TT 44	MP					8.04		
Kalloni, massive layered gabbros								
Ti 65	MG			6.62 ± 0.21 (2)				
Kionia Hill, gabbro blocks								
Ti 55	MG			6.64 ± 0.08 (2)		10.56	Hbl -49.7	
Ti 59	MG	6.96 ± 0.06 (2)	6.77 ± 0.03 (2)	8.96 ± 0.02 (2)	10.76	Fld 14.59 ± 0.07 (2)	Hbl -67.1	
Ti 58	MG	7.44 ± 0.09 (4)	6.65 ± 0.01 (2)	8.42 ± 0.16 (2)	10.18	Fld 14.91 ± 0.11 (4)	Hbl -67.7	
TK 131	AC			8.82				
TK 190	MP					11.72	Act -54.6	
Kalloni, gabbro blocks								
Ti 72	MG	6.69		6.25 ± 0.11 (2)		8.06	Hbl -60.6	
TM 209	MG	5.60 ± 0.09 (2)			10.19 ± 0.01 (2)			
Ti 76	MG						Hbl -57.0 ± 2.8 (2)	
Ti 73	MP					9.91		
TM 112	MP					9.88		
TM 212	MP					10.52		

Rock types: AC, actinolite–chlorite rock (metasomatic); FV, felsic vein; MG, metagabbro; MP, mafic phyllite; QV, quartz-epidote-chlorite vein. Minerals: Act, actinolite; Ep, epidote; Fld, feldspar; Hbl, hornblende; Qtz, quartz. Number in parentheses is number of repeat analyses; stated precision is 1 S.D. or half of the average difference if  $n=2$ .

Micro-sampling at the sub-millimeter-scale was achieved using the thin saw technique or drilling with a 0.5 mm diamond drill bit. These techniques permitted separation between different mineral generations as indicated by microtextures. Care was taken to distinguish between minerals according to their texture, color, grain-size, habit and inclusion density.

The purity of mineral separates was optically checked under the binocular and petrographic microscope and by X-ray diffraction. Aliquots of separated minerals were analyzed for chemical composition using a JEOL JXA 8600 electron microprobe in Jerusalem.

Mineral and whole-rock powders were analyzed for their oxygen isotope composition in the laser fluorination system at the University of Wisconsin-Madison using a  $\text{CO}_2$  laser,  $\text{BrF}_5$  reagent, and a Finnigan-MAT 251 mass spectrometer [27]. Whole-rock powders were analyzed using an ‘air-lock’ sample chamber [28], which allows fluorination of each sample individually. The UWG-2 garnet standard was analyzed on each day of laser analysis. Daily averages were within the uncertainty of the recommended value  $\delta^{18}\text{O}=5.8 \pm 0.1$  ‰ (1 S.D.). All analyses were corrected to the UWG-2 standard and most of the samples were duplicated or triplicated. The deviation

from the mean for replicates is routinely better than  $\pm 0.1\text{‰}$ .

A vacuum line based on the zinc-reduction method [29] was used in the extractions for hydrogen isotope analyses. Sample size was 30–40 mg of mineral separate. Isotopic analyses were made on the SIRA II mass spectrometer at the Geological Survey of Israel. Analyses were corrected to SMOW with NBS-30 biotite ( $\delta D = -64\text{‰}$ ) and an internal phengite standard (230 Mica) with measured differences  $\Delta D_{(230 \text{ Mica} - \text{NBS-30 biotite})} = 17.3 \pm 2.3\text{‰}$ . Duplicate analyses suggest that the precision is better than 4‰ (Table 1).

Isotopic fractionation between two minerals  $X$  and  $Y$  is described by the notation:  $\Delta(X-Y) = \delta X - \delta Y \approx 1000 \ln \alpha(X-Y)$ , where  $\delta X$  is the isotopic composition of the mineral measured in ‰ relative to the SMOW standard.  $A(X-Y)$  refers to the coefficient in the mineral fractionation equation:  $1000 \ln \alpha(X-Y) = A(X-Y) \times 10^6 T^{-2}$ .

#### 4. Results

The oxygen isotope compositions of minerals (augite, hornblende, actinolite and feldspar) from the Tinos metagabbros are listed in Table 1. The variations in isotope composition are shown in Figs. 3 and 4. For reference, a bar is

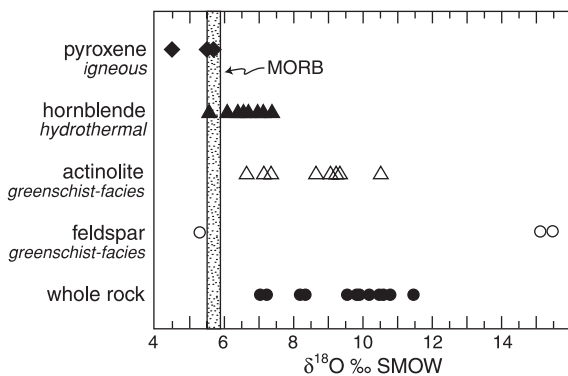


Fig. 3. The range of  $\delta^{18}\text{O}$  values of various minerals and whole rock of metagabbros from Tinos. The stippled band at  $\delta^{18}\text{O} = 5.7 \pm 0.2\text{‰}$  indicates the oxygen isotopic composition of unaltered igneous MORB.

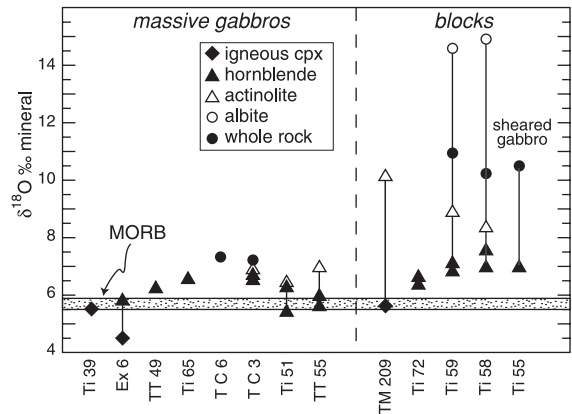


Fig. 4. Oxygen isotope ratios of minerals plotted from massive gabbros and gabbroic blocks. Minerals from blocks show heavier and more variable values.

shown indicating the compositional range of typical MORB whole rock.

Pyroxene separates from the Tinos gabbros have  $\delta^{18}\text{O}$  values of 5.3–5.7‰ (excluding sample EX 6, that is intruded by a felsic vein). These values are characteristic of primary igneous pyroxenes in oceanic gabbros [3,4]. The  $\delta^{18}\text{O}$  values of hornblende range from 5.5 to 7.4‰. This relatively restricted range is observed in both the massive metagabbros and the metagabbroic blocks (Fig. 4). No marked isotopic compositional differences are evident between the brown and green hornblendes. The actinolite and feldspar  $\delta^{18}\text{O}$  values plot in two groups. Actinolite in massive metagabbros has  $\delta^{18}\text{O}$  values in the range from 6.5 to 7.2‰. These values are close to, but slightly higher than, those of the hornblende that they replace (Fig. 4). In contrast, actinolites from metagabbroic blocks have significantly higher  $\delta^{18}\text{O}$  values, varying from 8.4 to 10.2‰. Similarly, albite in the metagabbroic blocks has high  $\delta^{18}\text{O}$  values of 14.6–14.9‰, whereas a felsic vein from a massive metagabbro has a low value of 5.3‰. Whole-rock  $\delta^{18}\text{O}$  values exhibit the same trends, with relatively low values ( $< 10\text{‰}$ ) in massive metagabbros and higher values (generally  $> 10\text{‰}$ ) values in the metagabbroic blocks.

The  $\delta D$  values of amphiboles and one epidote are given in Table 1 and plotted in Fig. 5. The  $\delta D$  values of hornblende fall in the range  $-69$ –

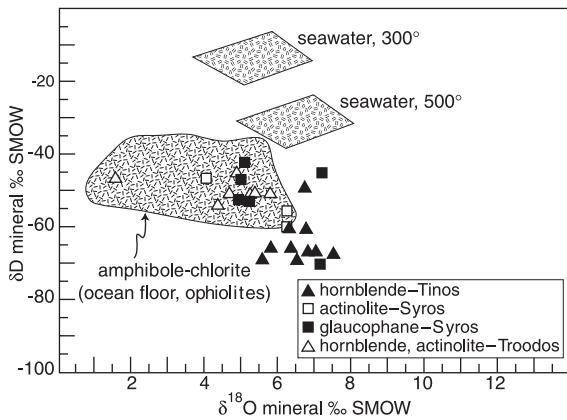


Fig. 5. A plot of the  $\delta D$  and  $\delta^{18}O$  values of Tinos hornblendes. Also shown are the isotopic compositions of actinolites and glaucophanes from Syros island [11]. The range of isotopic compositions of amphibole and chlorite reported from seafloor altered rocks and ophiolite suites is plotted for reference (data from [2,3,34,50]). Also shown are fields that correspond to the isotopic compositions of seawater in equilibrium with amphiboles of Troodos ophiolite gabbros at 300 and 500°C [34].

–50‰ and the one epidote separate gave a value of –59‰. Samples Ti 55, Ti 58 and Ti 59 are from the same metagabbroic block, the Kionia block, easily recognizable in the field (Fig. 2a). However, whereas samples Ti 58 and 59 with  $\delta D$  of hornblende = –67–68‰ are only moderately overprinted by greenschist-facies assemblages, sample Ti 55 is strongly overprinted and deformed, and gives a higher  $\delta D$  value of –50‰. An actinolite separate was also analyzed for one sample in this block (TK 190) and likewise yielded relatively high  $\delta D$  value of –55‰. These differences suggest that the greenschist overprint lead to D/H enrichment in minerals.

## 5. Discussion

### 5.1. Isotopic exchange during seafloor hydrothermal alteration of gabbros

The oxygen isotope ratios of hornblende are higher than expected for fresh mid-ocean ridge basalts (MORB) and gabbros that have undergone high-temperature seafloor alteration. This is clearly illustrated in Fig. 6, which compares

the range of  $\delta^{18}O$  values of the Tinos hornblendes with amphiboles from classical ophiolite suites such as Troodos and Samail (Oman), present-day oceanic gabbros, and relict seafloor amphiboles in the eclogite-facies metagabbros of Syros. The Tinos hornblendes are on the average 1.5–3.5‰ higher in  $\delta^{18}O$  than the other gabbros and do not show  $^{18}O/^{16}O$ -depleted compositions typical of high-temperature exchange with seawater.

The chemical composition of the Tinos hornblende is characteristic of hydrothermally altered mid-ocean ridge gabbros and indicates that it did not form as a primary igneous mineral [10,30,31]. Hornblende is observed to replace augite and is texturally secondary with respect to the igneous pyroxene. The oxygen isotope fractionation between hornblende and clinopyroxene is small ( $A(Hbl-Di) = 0.2 \pm 0.3$ ) [32] and typically  $\Delta(Hbl-Di) = 0.1-0.5$ ‰ in oceanic rocks [2]. However, the  $\delta^{18}O$  values of the Tinos hornblendes are approximately 1‰ higher than values found in the pyroxenes. For one sample in which

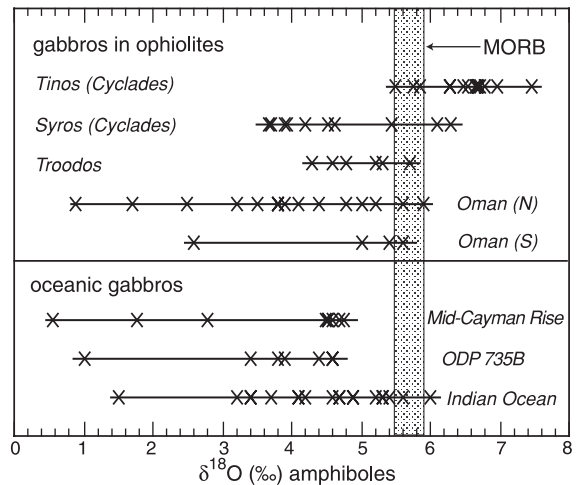


Fig. 6. Comparison between the  $\delta^{18}O$  values of hornblendes from Tinos metagabbros and the values reported for amphiboles of gabbros from ophiolites and present-day oceanic crust. The gray band at  $\delta^{18}O = 5.7 \pm 0.2$ ‰ indicates the oxygen isotopic composition of unaltered igneous MORB. Data sources are: Syros [11]; Troodos [34]; Northern Oman [45]; Southern Oman [1]; Mid-Cayman Rise [2]; ODP 735B [50]; Indian Ocean [3].

a mineral pair could be separated (EX 6),  $\Delta(\text{Hbl-Di}) = 1.37\text{‰}$ . This indicates that the hornblende did not grow in isotopic equilibrium with respect to the precursor pyroxene. It is not possible to exactly estimate the  $\delta^{18}\text{O}$  of the fluid from which the hornblende grew, since temperatures of hydrothermal alteration on the seafloor are not known and the hornblende–water fractionation has not been calibrated. An empirical estimate of the hornblende–water fractionation is given by combining the  $A(\text{Hbl-Di}) = 0.2$  [32] with the diopside–water fractionation [33]. Hornblende in submarine oceanic gabbros of the Mid-Cayman Rise forms within the temperature range 400–700°C [30]. Thus, the hornblende–water fractionation varies from  $\sim -0.4\text{‰}$  at 700°C to  $-0.9\text{‰}$  at 400°C. The isotopic composition of the water in equilibrium with the Tinos hornblende (average  $\delta^{18}\text{O} = 6.4 \pm 0.5\text{‰}$ ) at these temperatures could vary from approximately 6.5 to 8.0‰, i.e. it is significantly  $^{18}\text{O}/^{16}\text{O}$ -enriched relative to seawater with  $\delta^{18}\text{O} \approx 0\text{‰}$ .

Moderate- to high-temperature oxygen isotopic exchange between seawater and mafic plutonic rocks of primary igneous composition results in  $^{18}\text{O}/^{16}\text{O}$  depletion of the rocks and  $^{18}\text{O}/^{16}\text{O}$  enrichment of the seawater [1,34,35]. However, as has been noted above, the  $\delta^{18}\text{O}$  values of the Tinos hornblende are higher than those considered representative of ocean floor rocks (Fig. 6) and correspondingly, the  $\delta^{18}\text{O}$  of the water is higher than that typically found in such alteration. These data imply that the  $\delta^{18}\text{O}$  of the seawater that interacted with the Tinos gabbros was previously modified by high-temperature water–rock interaction. The D/H results may shed further light on exchange process because  $\delta D$  values are sensitive to change at low amounts of exchange or water/rock (W/R) ratios. On the  $\delta D$  vs.  $\delta^{18}\text{O}$  plot (Fig. 5), the Tinos hornblendes are slightly lower in  $\delta D$  and slightly higher in  $\delta^{18}\text{O}$  than typically observed in the amphiboles formed by seafloor alteration. This implies that the  $\delta D$  value of the water involved in the Tinos alteration was more negative than that involved in ‘typical’ seafloor alteration. Fig. 5 also shows the isotopic compositions of seawater produced during hydrothermal exchange of the Troodos ocean floor at 300 and 500°C [34].

These waters are both lower in  $\delta D$  and higher in  $\delta^{18}\text{O}$  than unaltered seawater and qualitatively fit the compositional ‘profile’ of the water that could produce the  $\delta D$  and  $\delta^{18}\text{O}$  values of the Tinos hornblendes by water–rock exchange. Thus, both the  $\delta D$  and  $\delta^{18}\text{O}$  data indicate that the water involved in the Tinos alteration had previously been exchanged by moderate- to high-temperature seafloor exchange.

## 5.2. Mass balance model of oceanic isotopic exchange

Constraints on the thermal structure and magnitudes of fluid fluxes of the sub-seafloor hydrothermal system at which the  $^{18}\text{O}/^{16}\text{O}$ -enriched seawater and gabbros could have developed are illustrated by model calculations in Fig. 7. The model builds directly on the transport equations and assumptions of Dipple and Ferry [36] to compute the isotopic changes in seawater and gabbro for a given temperature gradient and path length across the oceanic crust, assuming local equilibrium at different time-integrated fluid fluxes ([36], equation 9, [37]).

Our model assumes that isotopic exchange between seawater and gabbros occurs during the formation (and equilibration) of hornblende, at the 400–700°C temperature range [2,30]. The gabbro–water fractionation can be approximated by the plagioclase ( $\text{An}_{60}$ )–water fractionation:  $\Delta = 2.36 \times 10^6/T^2 - 3.24$  [38], because the chemical composition of  $\text{An}_{60}$  is quite close to that of Tinos metagabbros [10]. The plagioclase–water fractionation shows a crossover at high temperature: it is negative ( $\Delta = -0.75$ ) at 700°C, but positive ( $\Delta = 2.0$ ) at 400°C. We consider a two-stage flow path: (a) recharge of seawater into the gabbro column along a positive temperature gradient (heating) followed by (b) discharge of the isotopically altered seawater along a negative temperature gradient (cooling). The results of the calculations are shown on graphs of  $\delta^{18}\text{O}$  (water) and  $\delta^{18}\text{O}$  (gabbro) vs. depth (or temperature) within the gabbro section (Fig. 7a,b).

1. Recharge: The recharge path illustrates the effect of isotope exchange during downward

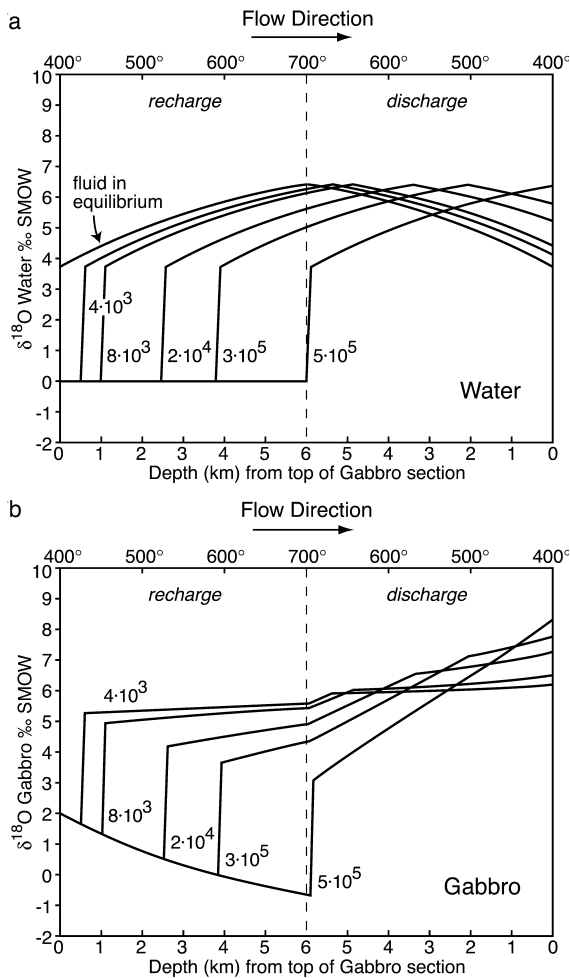


Fig. 7. Calculated change in  $\delta^{18}\text{O}$  of seawater (a) and gabbro (b) as a result of progressive isotopic exchange during flow of  $\text{H}_2\text{O}$  through gabbro along a linear temperature gradient of  $50^\circ\text{C}/\text{km}$  between 400 and  $700^\circ\text{C}$ . The calculation is based on the model for fluid flow and stable isotope alteration of Dipple and Ferry ([36], equation 9). Curves are labeled with values of time-integrated fluid flux in mol fluid/cm<sup>2</sup> rock. Both figures (a, b) describe a two-stage flow path: in the left part of each figure recharge of seawater ( $\delta^{18}\text{O}_{\text{initial}} = 0\text{‰}$ ) into a 6 km gabbro column ( $\delta^{18}\text{O}_{\text{initial}} = 5.7\text{‰}$ ) along a heating, positive temperature gradient is modeled. This is followed by discharge of the isotopically altered seawater along a cooling, negative temperature gradient to the top of the gabbro section as shown in the right part. The curve labeled 'fluid in equilibrium' in (a) shows  $\delta^{18}\text{O}$  values of water in equilibrium with gabbro at static conditions, prior to infiltration.

movement of seawater (originally with  $\delta^{18}\text{O} = 0\text{‰}$ ) into a 6 km thick gabbro column with uniform initial  $\delta^{18}\text{O} = 5.7\text{‰}$  and along a linear temperature gradient of  $50^\circ\text{C}/\text{km}$  between 400 and  $700^\circ\text{C}$ . The initial water at  $Z \leq 0$  has isotopic composition 3.7‰ less than water in equilibrium with gabbro at  $400^\circ\text{C}$ . The higher the fluid flux, the deeper the initial 3.7‰ discontinuity (alteration front) in  $\delta^{18}\text{O}$  (water) propagates. At depths greater than the depth of the  $\delta^{18}\text{O}$  front, increasing temperature results in a gradual increase in  $\delta^{18}\text{O}$  (water) at all time-integrated fluid fluxes  $< 5 \times 10^5$  mol  $\text{H}_2\text{O}/\text{cm}^2$  rock. The final result of the isotopic exchange in the recharge path is a high-temperature fluid enriched in  $^{18}\text{O}/^{16}\text{O}$ , up to 6.4‰ at low fluxes. Correspondingly fluid flow results in  $^{18}\text{O}/^{16}\text{O}$  depletion of the rock to variable degrees, depending on the magnitude of the time-integrated fluid fluxes.

2. Discharge: The  $^{18}\text{O}/^{16}\text{O}$ -enriched water is then allowed to flow back to the top of the 6 km thick gabbro section and down the temperature gradient ( $50^\circ\text{C}/\text{km}$ ). Initially,  $\delta^{18}\text{O}$  (water) increases to a maximum value of  $\sim 6.4\text{‰}$  and then gradually begins to decrease as the effect of the lower-temperature (positive) gabbro–water fractionation becomes influential. The isotopic composition of the gabbro gradually increases until it reaches a maximum value of  $> 6\text{‰}$  at the end of the path flow ( $400^\circ\text{C}$ ). Significant isotopic enrichment of high-level gabbros to values of above 7‰ is indicated at fluxes  $\geq 2 \times 10^4$  mol  $\text{H}_2\text{O}/\text{cm}^2$  rock.

The overall conclusion of the modeling is that high-temperature exchange is an effective process for raising the  $\delta^{18}\text{O}$  of seawater infiltrating into and hydrating a gabbro. Discharge of the enriched seawater in a regime of decreasing temperature is a particularly effective process of raising the  $\delta^{18}\text{O}$  of the gabbro to  $> 6\text{‰}$  at time-integrated fluid fluxes  $> 4 \times 10^3$  mol/cm<sup>2</sup>. The degree of enrichment in the rock is dependent on the chosen path length and especially on the temperature range and gradient, due to the temperature dependence of the fractionation. Thus, the low-

temperature part of the discharge path will strongly influence the final  $\delta^{18}\text{O}$  value of the rock. For simplicity, we chose the same temperature gradient and path length for the recharge and discharge paths. However, hydrothermal systems in oceanic spreading centers are thought to consist of widespread recharge zones and focused discharge zones [39]. Thus, the down-temperature discharge path might be shorter and the thermal gradient steeper than in the recharge path (Fig. 8b), resulting in high  $\delta^{18}\text{O}$  gabbros at deeper levels. Kinetic control of oxygen isotope exchange during fluid–rock interaction is possible: amphibole and pyroxene exchange oxygen much slower than plagioclase [33,40], and consequently their  $^{18}\text{O}/^{16}\text{O}$  enrichments will lag behind. We found that the results reported here would not be significantly different if hornblende–water or pyroxene–water fractionations were alternatively used. Yet, higher fluxes are needed to shift the isotopic composition of the rock.

The  $^{18}\text{O}/^{16}\text{O}$  enrichments in Tinos gabbros could have occurred in a process similar to the one modeled here. In that case they represent only the discharge path of the hydrothermal cell described by the model.

### 5.3. Tectonic environment of seafloor hydrothermal alteration

High  $\delta^{18}\text{O}$  values (or the lack of  $^{18}\text{O}/^{16}\text{O}$  depletion) in the upper plutonic level have been observed in a number of oceanic rocks: San Luis Obispo and Del Puerto ophiolite fragments in California [35,41]; Macquarie Island [42]; veins in Hole 504B [43]; gabbros from the Mathematician Ridge [31]. The data are largely determined for plagioclase and whole-rock samples, where later low-temperature exchange might potentially be responsible for  $^{18}\text{O}/^{16}\text{O}$  enrichment [44]. Notwithstanding, Gregory and Taylor [1] reported high  $\delta^{18}\text{O}$  values for the pyroxenes (4–8‰) of gabbroic dikes in the lower crustal section of the Oman ophiolite, to account for which they and Alt [39] proposed isolated, very hot, low seawater/rock ratio, hydrothermal cells beneath part of the axial magma chamber.

Stakes and Taylor [45] found that in all three

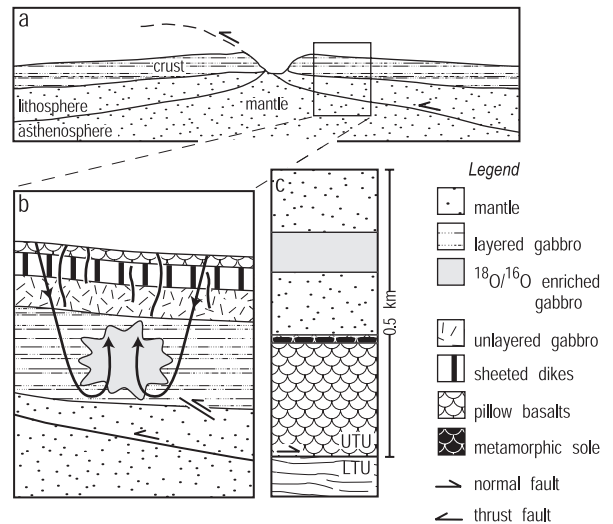


Fig. 8. Diagram illustrating the proposed tectonic setting for the oceanic fluid–rock interaction and the following regional metamorphism. a: Inter-oceanic thrusting of young and hot ophiolitic slab. b: Smaller-scale faulting and fracturing within the hanging-wall of the principle thrust allows penetration of seawater to deep, layered gabbros of the hot oceanic lithosphere. Gabbro–water oxygen exchange in a regime of increasing temperature results in  $^{18}\text{O}/^{16}\text{O}$  enrichment of the hydrothermal fluid, which in turn induces crystallization of  $^{18}\text{O}/^{16}\text{O}$ -enriched hornblende in gabbros during the discharge path. c: A schematic columnar section of the UTU on Tinos. The UTU includes a duplicated ophiolitic sequence with serpentized peridotite slices overlying metagabbro and metabasalt. Tectonic duplication occurred during inter-oceanic thrusting suggested by remnants of dynamic metamorphic aureole ('metamorphic sole') at the top of the basaltic slice. Whole-crust extension commenced at Late Oligocene times and involved significant attenuation of the ophiolite slices. The UTU was juxtaposed on top of exhumed HP rocks (LTU) during greenschist-facies overprint at the Early Miocene.

transects they made through the Samail ophiolite, the highest  $\delta^{18}\text{O}$  plagioclase (7–12‰) occurred in deep-seated gabbro located near the Moho. Since the elevated  $\delta^{18}\text{O}$  values were confined to plagioclase ( $\delta^{18}\text{O}$  (Hbl, Cpx) = 5.7‰), and the association of this enrichment with low-temperature hydrous minerals like prehnite and zeolite, they concluded that late stage high- $\delta^{18}\text{O}$  aqueous fluids penetrated the deepest gabbros. This fluid movement was related to 'structural dislocation' near the Moho, suggested by shear zones in the peridotite below the Moho [46] and connected to

thrusting at the base of the whole ophiolite slab [45]. The tectonic disruption caused fracturing that enabled penetration of high- $\delta^{18}\text{O}$  fluids. The short time interval between igneous crystallization of the Samail ophiolite and subsequent inter-oceanic thrusting (1–4 Ma) and granulite-facies metamorphism in the underlying metamorphic sole indicate obduction of very young and hot oceanic slab [47]. Thus, the inferred influx of aqueous fluids to the layered gabbros may have begun at high temperatures soon after the gabbros were able to sustain open fractures. Compared to the relatively intact ophiolite in Oman, the Tinos ophiolite exposures provide good field evidence for inter-ophiolitic (oceanic) thrusting. Deep, layered gabbro overlies serpentinite, which overlies mafic phyllites (metabasalts) in the Tsiknias exposure, and gabbro overlies mafic phyllites in the Cape Stavros exposure. Highly-tectonized amphibolite associated with a shear zone at the base of the ultramafic slice in Tsiknias was interpreted as a relict of a metamorphic sole formed by hot thrusting of a young ophiolite slab over mafic oceanic rocks [10]. Correspondingly, it is suggested that the evidence for early, high-temperature near-axis intra-oceanic thrusting, fracturing and infiltration that is required by the Stakes and Taylor model [45], is found in the isotopic data of the Tinos hornblende.

Cross-sections illustrating the fluid infiltration process are shown in Fig. 8. Near-axis thrusting enabled infiltration of high- $\delta^{18}\text{O}$  fluids to the deep-seated layered gabbros (Fig. 8a,b). The thick crustal section through which these fluids must have penetrated enabled prolonged O exchange, raising the  $\delta^{18}\text{O}$  of the water. Temperature increases with downward fluid movement into the deeper gabbroic section and therefore isotopic exchange and  $^{18}\text{O}/^{16}\text{O}$  enrichment in the water is best approximated by the 400–700°C recharge path calculation given in Fig. 7a. The  $^{18}\text{O}/^{16}\text{O}$ -enriched water then flowed upward in discharge zones to enrich gabbros in progressively decreasing temperatures as modeled in Fig. 7b. The calculation requires an earlier up-temperature isotopic exchange zone in which  $\delta^{18}\text{O}$  (water) increases but the gabbro becomes  $^{18}\text{O}/^{16}\text{O}$ -depleted relative to its initial value of 5.7‰. As

noted, this section is not seen at Tinos, but is found in the metamorphosed ophiolite exposures on Syros. The exposures of the Tinos upper unit were shown to represent a sliced and dismembered ophiolite complex: ultramafic, gabbroic and basaltic members are represented on Tinos, but other components, such as the sheeted dykes and the sedimentary cover, are missing [10]. The thickness of the exposed sections on Tinos is also smaller by one or two orders of magnitude than found in complete ophiolite sections. It is therefore suggested that  $^{18}\text{O}/^{16}\text{O}$ -depleted rocks were originally present on Tinos, but were tectonically removed during the emplacement and subsequent thinning due to extensional tectonics (Fig. 8c).

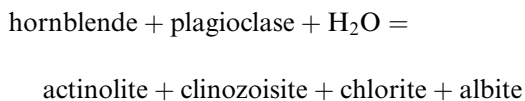
The  $^{18}\text{O}/^{16}\text{O}$ -enriched Tinos gabbros stand in distinct contrast to the high-pressure metagabbros on Syros, which preserve low  $\delta^{18}\text{O}$  sub-seafloor alteration values. The simplest explanation for this difference is that the Tinos and Syros metagabbros represent different segments of the Pindos ocean floor that have undergone different seafloor alteration. In this respect, the Syros metagabbros would represent ‘typical’ seafloor alteration and the Tinos metagabbros a different environment, affected by early, inter-oceanic thrusting. The metabasalts of both the upper and lower tectonic units on Tinos, however, preserve the high  $\delta^{18}\text{O}$  values (typically > 10‰) representative of low-temperature seafloor alteration [10,11,26].

#### 5.4. Isotopic exchange during the orogenic stage

A marked feature of the oceanic alteration stage was that similar  $\delta^{18}\text{O}$  and  $\delta D$  values were observed in the hornblende of both massive layered metagabbros and meter-sized metagabbroic blocks (Fig. 4). This is not the case with minerals that grew during the regional greenschist metamorphic overprint that occurred during the orogenic stage of evolution, as the result of either thrusting and piling up of nappes during obduction or ductile shear during extension [10,22,24,25]. Distinctly higher  $\delta^{18}\text{O}$  values are observed for greenschist minerals (actinolite, albite) in the metagabbroic blocks compared to the values for these minerals in massive metagabbros (Fig. 4). A slight increase in  $\delta D$  of amphi-

boles has also been inferred in one of the blocks strongly overprinted by the greenschist metamorphism.

The actinolites in massive metagabbros have  $\delta^{18}\text{O}$  values (6.5–7.0‰) that are close to those of hornblende. In the three samples for which both hornblende and actinolite overgrowth were analyzed,  $\Delta(\text{Act-Hbl})$  varies from 0.3 to 1‰. This compares with the equilibrium actinolite–hornblende fractionation of  $\sim 0.2$  at 575°C [32], which implies an equilibrium fractionation of  $\sim 0.3$  at greenschist-facies temperatures of 400–450°C. Thus, the measured  $\Delta(\text{Act-Hbl})$  values approximate the equilibrium value. The greenschist overprint can be represented by the reaction:



The stoichiometric hydration reaction requires the addition of a small amount of water ( $\sim 1$  wt% of the rock). This small amount of water would not change the isotopic composition of the whole-rock assemblage, thus allowing actinolite to form in or near oxygen isotope equilibrium with the hornblende. The slight disequilibrium fractionation in two samples, however, indicates that a small amount of high- $\delta^{18}\text{O}$  fluid has also penetrated the rocks as well and influenced the isotopic composition of the actinolite.

Albite and actinolite of the greenschist-facies overprint in the metagabbroic blocks have high  $\delta^{18}\text{O}$  values (9–15‰) and clearly developed in isotopic disequilibrium with the hornblende and in the presence of relatively high- $\delta^{18}\text{O}$  water. The isotopic fractionation in samples Ti 58 and 59,  $\Delta(\text{Ab-Act}) = 5.6\text{--}6.5\text{‰}$ , is much larger than the expected equilibrium fractionation at peak metamorphic temperatures ( $\Delta(\text{Ab-Act}) = 2.7\text{‰}$  at 400°C). A plausible explanation for this disequilibrium is resetting of  $\delta^{18}\text{O}$  (albite) by exchange with water during cooling below peak metamorphic temperatures. An estimate of the isotopic composition of this water is obtained from  $\delta^{18}\text{O}$  values of 14.6 and 14.9‰ for the albite separated from samples Ti 58 and 59. At post-peak temperatures of 300–350°C, the al-

bite–water fractionation is 6–4.5‰ [38], thus implying  $\delta^{18}\text{O}$  (water) of 8.5–10.5‰. The host rocks of the blocks are mainly mafic phyllites with  $\delta^{18}\text{O}$  values in the range 11–12.5‰ [10]. The calculated  $\delta^{18}\text{O}$  of the water in equilibrium with these phyllites at 300–350°C is in the range 7–10‰ (calculated as for gabbro using the plagioclase ( $\text{An}_{60}$ )–water fractionation). Thus, the most likely source of the high- $\delta^{18}\text{O}$  fluid in the overprint of the metagabbroic blocks is dehydration of the surrounding mafic phyllites. The high  $\delta^{18}\text{O}$  of mafic phyllites indicates that precursor basalts had undergone low-temperature seafloor alteration and hydration. During the greenschist metamorphism, these rocks would have undergone dehydration.

Deformation is a major factor controlling the difference in scale of fluid–rock interaction exhibited by the two gabbro types. The metagabbroic blocks are meter-size or less, deformed and more strongly overprinted by the greenschist metamorphism (Fig. 2a). In comparison, the massive layered metagabbro sequences are thicker (5–20 m), still preserve igneous textures, and are much less overprinted. Deformation as a controlling factor of permeability enhancement is well known from isotopic studies of shear zones ([48] and references cited therein). In the Tinos metagabbros, the deformation was stronger in the smaller blocks, and the permeability created during this deformation facilitated the greater degree of fluid infiltration and greenschist overprint in these rocks.

## 6. Conclusions

The metagabbros of Tinos form part of a dismembered ophiolitic sequence that records processes of oceanic hydrothermal alteration as well as regional greenschist-facies metamorphism during orogenesis. Laser fluorination analyses show that these metagabbros are characterized by unusually high  $\delta^{18}\text{O}$  values of minerals and rocks and allow the distinction between hydrothermal and regional metamorphic water–rock interaction.

The hydrothermal alteration pattern of the Tinos gabbroic section is more complicated than predicted from previous studies, and presumably

reflects the complexity of hydrothermal flow within the deeper oceanic crust [1,39,45,49]. The  $\delta^{18}\text{O}$  of hornblende reflects high-temperature hydrothermal alteration of gabbro by  $^{18}\text{O}/^{16}\text{O}$ -enriched seawater. Taking into account the *D/H* compositions of hornblendes and modeling of fluid–rock interaction, it is suggested that progressive  $^{18}\text{O}/^{16}\text{O}$  enrichment in the seawater-derived hydrothermal fluid occurred as the result of gabbro–water exchange in a regime of increasing temperature. Near-axis thrusting and fracturing enabled infiltration of high- $\delta^{18}\text{O}$  fluids to the deep-seated layered gabbros. The buoyant fluids rose upward in discharge zones and enriched the gabbros. This model of fluid–rock interaction implies that a zone of  $^{18}\text{O}/^{16}\text{O}$ -depleted rocks was also present at the time of hydrothermal alteration. Such a section of  $^{18}\text{O}/^{16}\text{O}$ -depleted metaigneous rocks is, however, absent in the Tinos ophiolite section and it is suggested that it was tectonically removed from the original ophiolitic suite, possibly during obduction and emplacement and subsequent thinning due to extensional tectonics.

The isotope ratios of the metagabbros acquired during the hydrothermal alteration were subsequently modified by the regional greenschist-facies metamorphism, which produced  $^{18}\text{O}/^{16}\text{O}$  enrichment in the greenschist-facies minerals (actinolite and albite). The greenschist-facies overprint only slightly affected the massive layered gabbros, but strong  $^{18}\text{O}/^{16}\text{O}$  enrichment was observed in isolated blocks. The host rocks to the gabbro blocks are ocean floor basalts that underwent  $^{18}\text{O}/^{16}\text{O}$  enrichment during low-temperature alteration on the seafloor. Dehydration reactions accompanying their metamorphism thus provided the high- $\delta^{18}\text{O}$  infiltrating fluid, and deformation undoubtedly assisted the infiltration through the creation of deformation-enhanced permeability.

### Acknowledgements

We thank Mike Spicuzza for assistance with oxygen isotope analyses and technical support in general and Brian Hess for help with sample preparation. Lukas Baumgartner is thanked for helpful discussion of fluid flow modeling. Hydrogen

isotope mass-spectrometry was performed by Dr A. Ayalon at the Geological Survey of Israel. B.P. also thanks Mike Spicuzza for his help during her visits in Madison. This work was supported by a grant from the United States–Israel Binational Science Foundation (BSF), Jerusalem. The stable isotope laboratory at the University of Wisconsin is supported by NSF, EAR 96-28260 and DOE 93 ER14389. We are grateful to Mike Bickle and Colin Graham for thoughtful reviews that significantly improved this paper. Y.K. is supported by an Albert and Alice Weeks post-doctoral fellowship of the Department of Geology and Geophysics, University of Wisconsin, Madison. [BW]

### References

- [1] R.T. Gregory, H.P. Taylor, An oxygen isotope profile in a section of Cretaceous oceanic crust, Samail Ophiolite, Oman: evidence for  $\delta^{18}\text{O}$  buffering of the oceans by deep (>5 km) seawater-hydrothermal circulation at mid-ocean ridges, *J. Geophys. Res.* 86 (1981) B2737–B2755.
- [2] E. Ito, R.N. Clayton, Submarine metamorphism of gabbros from the Mid-Cayman Rise: an oxygen isotopic study, *Geochim. Cosmochim. Acta* 47 (1983) 535–546.
- [3] D. Stakes, Oxygen and hydrogen isotope compositions of oceanic plutonic rocks: High temperature deformation and metamorphism of oceanic layer 3, in: H.P. Taylor, J.R. O'Neil, I.R. Kaplan (Eds.), *Stable Isotope Geochemistry: A Tribute to Samuel Epstein*, *Geochem. Soc. Spec. Publ.* 3, 1991, pp. 77–90.
- [4] E.H. Talbi, J. Honnorez, N. Clauer, F. Gauthier-Lafay, P. Stille, Petrology, isotope geochemistry and chemical budgets of oceanic gabbros-seawater interactions in the Equatorial Atlantic, *Contrib. Mineral. Petrol.* 137 (1999) 246–266.
- [5] J.M. Eiler, P. Schiano, N. Kitchen, E.M. Stolper, Oxygen-isotope evidence for recycled crust in the sources of mid-ocean-ridge basalts, *Nature* 403 (2000) 530–534.
- [6] K. Muehlenbachs, Alteration of the oceanic crust and the  $^{18}\text{O}$  history of seawater, in: J.W. Valley, H.P. Taylor, J.R. O'Neil (Eds.), *Stable Isotopes in High Temperature Geological Processes*, *Mineralogical Society of America, Rev. Mineral.* 16, 1986, pp. 425–444.
- [7] M. Bonneau, Correlation of the Hellenide nappes in the south-east Aegean and their tectonic reconstruction, in: J.E. Dixon, A.H.F. Robertson (Eds.), *The Geological Evolution of the Eastern Mediterranean*, *Geol. Soc. Spec. Publ.* 17, London, 1984, pp. 517–528.
- [8] D.J. Papanikolaou, Tectonic evolution of the Cycladic blueschist belt (Aegean Sea, Greece), in: H.C. Helgeson (Ed.), *Chemical Transport in Metasomatic Processes*,

- NATO ASI Ser. 218 C, Reidel, Dordrecht, 1987, pp. 429–450.
- [9] J.E. Dixon, J.R. Ridley, Syros, in: H.C. Helgeson (Ed.), *Chemical Transport in Metasomatic Processes*, NATO ASI Ser. 218 C, Reidel, Dordrecht, 1987, pp. 489–501.
- [10] Y. Katzir, A. Matthews, Z. Garfunkel, M. Schliestedt, D. Avigad, The tectono-metamorphic evolution of a dismembered ophiolite (Tinos, Cyclades, Greece), *Geol. Mag.* 133 (1996) 237–254.
- [11] B. Putlitz, A. Matthews, J.W. Valley, Laser-probe oxygen isotope study of high pressure metagabbros and metabasalts (Cyclades, Greece): Implications for subduction processes, *Contrib. Mineral. Petrol.* 138 (2000) 114–126.
- [12] M. Bröcker, A. Kreuzer, A. Matthews, M. Okrusch,  $^{40}\text{Ar}/^{39}\text{Ar}$  and oxygen isotope studies of polymetamorphism from Tinos Island, Cycladic blueschist belt, Greece, *J. Metamorph. Geol.* 11 (1993) 223–240.
- [13] M. Bröcker, M. Enders, U-Pb zircon geochronology of unusual eclogite-facies rocks from Syros and Tinos (Cyclades, Greece), *Geol. Mag.* 136 (1999) 111–118.
- [14] S. Dürr, Das Attisch-Kykladische Krystallin, in: V. Jacobshagen (Ed.), *Geologie von Griechenland*, Bornträger, Berlin, 1986, pp. 116–148.
- [15] Y. Katzir, D. Avigad, A. Matthews, Z. Garfunkel, B.W. Evans, Origin, HP/LT metamorphism and cooling of ophiolitic mélanges in southern Evia (NW Cyclades), Greece, *J. Metamorph. Geol.* 18 (2000) 699–718.
- [16] M. Schliestedt, Eclogite-blueschist relationships evident by mineral equilibria in the high-pressure metabasic rocks of Sifnos (Cycladic islands), *J. Petrol.* 27 (1986) 1437–1459.
- [17] A. Matthews, Oxygen isotope geothermometers for metamorphic rocks, *J. Metamorph. Geol.* 12 (1994) 211–220.
- [18] D. Avigad, A. Matthews, B.W. Evans, Z. Garfunkel, Cooling during the exhumation of a blueschist terrane: Sifnos (Cyclades), Greece, *Eur. J. Mineral.* 4 (1992) 619–634.
- [19] M. Patzak, M. Okrusch, H. Kreuzer, The Akrotiri Unit on the island of Tinos, Cyclades, Greece: Witness to a lost terrane of Late Cretaceous age, *N. Jb. Geol. Paläont. Abh.* 194 (1994) 211–252.
- [20] D. Avigad, Z. Garfunkel, Low-angle faults above and below a blueschist belt - Tinos island, Cyclades, *Terra Nova* 1 (1989) 182–187.
- [21] D. Avigad, Z. Garfunkel, L. Jolivet, J.M. Azañon, Back arc extension and denudation of Mediterranean eclogites, *Tectonics* 16 (1997) 924–941.
- [22] J. Stolz, M. Engi, M. Rickli, Tectonometamorphic evolution of SE Tinos, Cyclades, Greece, *Schweiz. Mineral. Petrogr. Mitt.* 77 (1997) 209–231.
- [23] L. Jolivet, M. Patriat, Ductile extension and the formation of the Aegean Sea, in: B. Durand, L. Jolivet, F. Horváth, M. Séranne (Eds.), *The Mediterranean Basins: Tertiary Extension within the Alpine Orogen*, *Geol. Soc. Spec. Publ.* 156, London, 1999, pp. 427–456.
- [24] M. Bröcker, L. Franz, Rb-Sr isotope studies on Tinos Island (Cyclades, Greece): additional time constraints for metamorphism, extent of infiltration-controlled overprinting and deformational activity, *Geol. Mag.* 135 (1998) 369–382.
- [25] S. Zeffren, D. Avigad, A. Heimann, Dating the displacement and deformation along a low-angle normal fault in the Cycladic islands, Greece, in: *Israel Geol. Soc. Ann. Meeting*, 2000, 134.
- [26] J. Ganor, A. Matthews, M. Schliestedt, Z. Garfunkel, Oxygen isotope heterogeneities of metamorphic rocks: an original tectonostratigraphic signature, or an imprint of exotic fluids? A case study of Sifnos and Tinos islands (Greece), *Eur. J. Mineral.* 8 (1996) 719–732.
- [27] J.W. Valley, N. Kitchen, M.J. Kohn, C.R. Niendorf, M.J. Spicuzza, UWG-2, a garnet standard for oxygen isotope ratios: Strategies for high precision and accuracy with laser heating, *Geochim. Cosmochim. Acta* 59 (1995) 5523–5534.
- [28] M.J. Spicuzza, J.W. Valley, V.S. McConnell, Oxygen isotope analyses of whole rocks via laser fluorination: an air lock approach, *Geol. Soc. Am. Abstr. Prog.* 30 (1998) 80.
- [29] T.W. Venneman, J.R. O'Neil, A simple and inexpensive method of hydrogen isotope and water analyses of minerals and rocks based on zinc reagent, *Chem. Geol.* 103 (1993) 227–234.
- [30] E. Ito, A.T. Anderson, Submarine metamorphism of gabbros from Mid-Cayman Rise: petrographic and mineralogical constraints on hydrothermal processes at slow-spreading ridges, *Contrib. Mineral. Petrol.* 82 (1983) 371–388.
- [31] D.S. Stakes, D.A. Vanko, Multistage hydrothermal alteration of gabbroic rocks from the failed Mathematician Ridge, Earth Planet. Sci. Lett. 79 (1986) 75–92.
- [32] M.J. Kohn, J.W. Valley, Oxygen isotope geochemistry of the amphiboles: Isotope effects of cation substitutions in minerals, *Geochim. Cosmochim. Acta* 62 (1998) 1947–1958.
- [33] A. Matthews, J.R. Goldsmith, R.N. Clayton, Oxygen isotopic fractionations involving the pyroxenes: The calibration of mineral-pair geothermometers, *Geochim. Cosmochim. Acta* 47 (1983) 631–644.
- [34] T.H.E. Heaton, S.M.F. Sheppard, Hydrogen and oxygen isotope evidence for sea-water hydrothermal alteration and ore deposition, Troodos Complex, Cyprus, in: *Volcanic Processes in Ore Genesis*, *Geol. Soc. Spec. Publ.* 7, London, 1977, pp. 42–57.
- [35] P. Schiffman, A. Williams, R. Evarts, Oxygen isotope evidence for submarine hydrothermal alteration of the Del Puerto ophiolite, California, *Earth Planet. Sci. Lett.* 70 (1984) 207–220.
- [36] G.M. Dipple, J.M. Ferry, Fluid flow and stable isotope alteration in rocks at elevated temperatures with applications to metamorphism, *Geochim. Cosmochim. Acta* 56 (1992) 3539–3550.
- [37] L.P. Baumgartner, D. Rumble, Transport of stable isotopes. I: Development of a kinetic continuum theory for stable isotope transport, *Contrib. Mineral. Petrol.* 98 (1988) 417–430.

- [38] J.R. O'Neil, H.P. Taylor, The oxygen isotope and cation exchange chemistry of feldspars, *Am. Mineral.* 52 (1967) 1414–1437.
- [39] J.C. Alt, Subseafloor processes in mid-ocean ridge hydrothermal systems, in: S.E. Humphris, R.A. Zierenberg, L.S. Mullineaux, R.E. Thomson (Eds.), *Seafloor Hydrothermal Systems: Physical, Chemical, Biological, and Geological Interactions*, American Geophysical Union, *Geophys. Monogr.* 91, 1995, pp. 85–114.
- [40] D.R. Cole, S. Chakraborty, Rates and mechanisms of isotopic exchange, in: J.W. Valley, D.R. Cole (Eds.), *Stable Isotope Geochemistry*, Mineralogical Society of America, *Rev. Mineral. Geochem.* 43 (2001) 83–224.
- [41] M. Magaritz, H.P. Taylor, Oxygen, hydrogen, and carbon isotope studies of the Franciscan Formation, Coast Ranges, California, *Geochim. Cosmochim. Acta* 40 (1976) 215–234.
- [42] J.D. Cocker, B.J. Griffin, K. Muehlenbachs, Oxygen and carbon isotope evidence for seawater hydrothermal alteration of the Maquarie Island ophiolite, *Earth Planet. Sci. Lett.* 61 (1982) 112–122.
- [43] J. Alt, J. Honnorez, C. Laverne, R. Emmermann, Hydrothermal alteration of a 1 km section through the upper oceanic crust, Deep Sea Drilling Project Hole 504B: mineralogy, chemistry, and evolution of seawater-basalt interaction, *J. Geophys. Res.* 91 (1986) B10309–B10335.
- [44] T.J. Barrett, H. Friedrichsen, Stable isotope composition of atypical ophiolitic rocks from east Liguria, Italy, *Chem. Geol.* 80 (1989) 71–84.
- [45] D. Stakes, H.P. Taylor, The northern Semail ophiolite: an oxygen isotope, microprobe, and field study, *J. Geophys. Res.* 97 (1992) 7043–7080.
- [46] F. Boudier, J.L. Bouchez, A. Nicolas, M. Cannat, G. Ceuleneer, M. Misseri, R. Montigny, Kinematics of oceanic thrusting in the Oman ophiolite: model of plate convergence, *Earth Planet. Sci. Lett.* 75 (1985) 215–222.
- [47] B.R. Hacker, J.L. Mosenfelder, E. Gnos, Rapid emplacement of the Oman ophiolite; thermal and geochronological constraints, *Tectonics* 15 (1996) 1230–1247.
- [48] A. Matthews, J. Liebermann, D. Avigad, Z. Garfunkel, Fluid-infiltration accompanying thrusting in an Alpine Metamorphic Complex (Tinos island, Greece), *Contrib. Mineral. Petrol.* 135 (1999) 212–224.
- [49] P. Schiffman, B. Smith, Petrology and oxygen isotope geochemistry of a fossil seawater hydrothermal system within the Solea Graben, northern Troodos Ophiolite, Cyprus, *J. Geophys. Res.* 93 (1988) B4612–B4624.
- [50] P.D. Kempton, C.J. Hawkesworth, C.J. Fowler, Geochemistry and isotopic compositions of gabbros from Layer 3 of the Indian Ocean crust, Hole 735B, *Proc. Ocean Drill. Prog. Sci. Res.* 118 (1991) 127–142.